Recovery of reduced thiol groups by superoxide-mediated denitrosation of nitrosothiols

Stefan Schildknecht [a],[**], Alex von Kriegsheim [b], Ksenija Vujacic-Mirski [c], Fabio Di Lisa [d], Volker Ullrich [f], Andreas Daiber [c],[e],[*]

[a] *Albstadt-Sigmaringen University, Faculty of Life Sciences, 72488, Sigmaringen, Germany*
[b] *Institute of Genetics and Cancer, University of Edinburgh, UK*
[c] *Center for Cardiology, Department of Cardiology 1, Laboratory of Molecular Cardiology, University Medical Center of the Johannes Gutenberg University, 55131, Mainz, Germany*
[d] *Department of Biomedical Sciences, University of Padova, Padova, Italy*
[e] *Partner Site Rhine-Main, German Center for Cardiovascular Research (DZHK), Langenbeckstr. 1, 55131, Mainz, Germany*
[f] *Department of Biology, University of Konstanz, Germany*

ARTICLE INFO

ABSTRACT

Nitrosation of critical thiols has been elaborated as reversible posttranslational modification with regulatory function in multiple disorders. Reversibility of S-nitrosation is generally associated with enzyme-mediated one-electron reductions, catalyzed by the thioredoxin system, or by nitrosoglutathione reductase.

In the present study, we confirm previous evidence for a non-enzymatic de-nitrosation of nitrosoglutathione (GSNO) by superoxide. The interaction leads to the release of nitric oxide that subsequently interacts with a second molecule of superoxide ($O_2^{\bullet-}$) to form peroxynitrite. Despite the formation of peroxynitrite, approximately 40–70% of GSNO yielded reduced glutathione (GSH), depending on the applied analytical assay. The concept of $O_2^{\bullet-}$ dependent denitrosation was then applied to S-nitrosated enzymes. S-nitrosation of isocitrate dehydrogenase (ICDH; NADP$^+$-dependent) was accompanied by an inhibition of the enzyme and could be reversed by dithiothreitol. Treatment of nitrosated ICDH with $O_2^{\bullet-}$ indicated ca. 50% recovery of enzyme activity. Remaining inhibition was largely consequence of oxidative modifications evoked either by $O_2^{\bullet-}$ or by peroxynitrite. Recovery of activity in S-nitrosated enzymes by $O_2^{\bullet-}$ appears relevant only for selected examples. In contrast, recovery of reduced glutathione from the interaction of GSNO with $O_2^{\bullet-}$ could represent a mechanism to regain reducing equivalents in situations of excess $O_2^{\bullet-}$ formation, e.g. in the reperfusion phase after ischemia.

1. Introduction

S-nitrosation is a posttranslational oxidative modification of thiols, not only relevant for the formation of nitrosoglutathione (GSNO) and its role in transnitrosation, but even more so as regulatory element in cellular redox regulation [1–4]. S-nitrosation of proteins is typically associated with an inhibition of their regular function, as illustrated by a wide variety of biological targets such as impaired DNA binding of the NF-κB subunits p50 and p65 [5,6], or the inhibition of glyceraldehyde-3-phosphate dehydrogenase activity [7,8]. For mitochondrial procaspase-3, a high degree of S-nitrosation was reported, contributing to its inactivation under non-apoptotic conditions [9,10]. S-nitrosation of cyclophilin D, a critical mPTP mediator, attenuates mPTP opening and consequently protects from cell death [11,12]. Despite its obvious relevance in redox regulation, the precise mechanisms involved in the formation of S-nitrosothiols under cellular conditions are not fully resolved yet. Dinitrogen trioxide (N_2O_3) is considered as strong nitrosating agent. The nitrosonium ion [NO$^+$] reflects the active nitrosating species and can interact with thiolates, to yield S-nitrosothiols [13]. In the presence of concurrent $^{\bullet}$NO and

superoxide ($O_2^{\bullet-}$) fluxes, maximal formation of N_2O_3 was observed at a $^\bullet NO$: $O_2^{\bullet-}$ ratio of 3 : 1 [14] according to the equations:

1) $^\bullet NO + O_2^{\bullet-} + H^+ \rightarrow HOONO$
2) $HOONO + {}^\bullet NO \rightarrow {}^\bullet NO_2 + HONO$
3) $^\bullet NO_2 + {}^\bullet NO \rightarrow N_2O_3$

Autoxidation of $^\bullet NO$ under aerobic conditions to form N_2O_3 has been proposed as alternative mechanism [15–18]. As this reaction is second order with respect to $^\bullet NO$, the reaction would be very slow, given the low steady-state concentrations of $^\bullet NO$ in biological systems [19]. More recent observations however suggest the formation of S-nitrosoglutathione at submicromolar $^\bullet NO$ fluxes under aerobic conditions in the presence of millimolar concentrations of reduced glutathione. This indicates quantitative nitrosation in the presence of physiological levels of $^\bullet NO$ under cellular conditions via the formation of a thiyl radical and its interaction with $^\bullet NO$ [20–23]. One precondition for classifying S-nitrosation as regulatory element in cellular redox regulation is its reversibility. In fact, distinct enzymatic denitrosation systems, such as S-nitrosoglutathione reductase, or the thioredoxin system, have been discovered [24]. Mitochondrial caspase 9 provides an excellent example for enzymatic de-nitrosation of a biological target that is directly associated with the re-activation of its protease activity in response to TNF-α-stimulation of a cell [9].

Enzymatic reversibility, as integral element of cellular redox regulation, has also been observed in association with the two-electron reduction of disulfides [25]. However, strong oxidants (e.g. peroxynitrite; Fe^{2+} +H_2O_2) can lead to modifications such as tyrosine nitration or to the formation of higher oxidation states of sulfur that are no longer subject of reversibility [26]. S-nitroso derivatives are not subject of further oxidation and hence could prevent from an irreversible formation of sulfins or sulfones from thiolates as observed e.g. in aldehyde dehydrogenase-2 (ALDH-2) [27,28]. Nitrosation conditions, succeeded by excessive $O_2^{\bullet-}$ fluxes, are hallmarks of ischemia reperfusion [29]. In this context, nitrosation and inactivation of mitochondrial Complex I has been identified as a protective mechanism by its inhibitory influence on the formation of large fluxes of reactive oxygen species by the respiratory chain in the initial stages of reperfusion [30–33]. During reperfusion, Complex I in fact displayed rapid de-nitrosation and re-activation, despite the described oxidative depletion of reducing equivalents (NADPH, NADH, GSH), thus limiting the contribution of enzymatic systems in the observed de-nitrosation and points to an additional mechanism involved [34]. The chemical structure of S-nitrosothiols prones this oxidative modification as potential target of non-enzymatic breakdown, as exemplarily represented by the transition metal-catalyzed cleavage of S-nitrosothiols [35–37]. In fact, several indications for $O_2^{\bullet-}$ mediated de-nitrosation of GSNO can be found in the literature [38–41].

On the basis of these observations, the present work investigates the hypothesis of $O_2^{\bullet-}$ as non-enzymatic mechanism for the denitrosation of S-nitrosothiols in order to regain *a)* GSH from GSNO and *b)* the reduced thiol state to recover activity of inactivated thiol-dependent enzymes.

2. Materials and methods

2.1. Oxidative denitrosation of GSNO and assessment of nitration of bovine serum albumin

GSNO (100 μM) was incubated with increasing concentrations (0.02–20 mU/ml) of xanthine oxidase (EC 1.1.3.22, grade III from buttermilk) from Sigma-Aldrich (Deisenhofen, Germany) for 45 min at 37 °C. Likewise, a fixed concentration of XO (4 mU/ml) was incubated with increasing concentrations of GSNO (0.5–500 μM). The reaction buffer (PBS) contained 1 mg/ml bovine serum albumin, 150 μM diethylenetriamine pentaacetate and 1 mM hypoxanthine. An aliquot of 50 μl was injected for HPLC analysis and another aliquot of 30 μl was used for dot blot analysis.

Analysis of protein tyrosine nitration was performed by dot blot as previously described [42,43]. Briefly, 50 μl (1 μg/μl stock) bovine serum albumin was transferred to a Protran BA85 (0.45 μm) nitrocellulose membrane (Schleicher & Schuell, Dassel, Germany) by a Minifold I vacuum Dot-Blot system (Schleicher & Schuell, Dassel, Germany). Each slot was washed twice with 200 μl PBS before and after protein transfer. The membrane was dried for 60 min at 60 °C. Equal loading of protein amounts per dot was then verified by staining the membrane with Ponceau S. Next, the membrane was incubated with blocking buffer and then primary antibody in blocking buffer according to the supplier's instructions. Protein tyrosine nitration was detected using a specific antibody for 3-NT (1:1,000, Anti-nitrotyrosine, rabbit immunoaffinity purified IgG, EMD Merck Millipore Corp, Merck KGaA, Darmstadt Germany). Positive bands were detected by enhanced chemiluminescence after incubation with a peroxidase-coupled secondary antibody (1: 5, 000, GAR-POX) (Vector Laboratories, CA, USA). Densitometric quantification of the dots was performed using the Super Signal ECL kit from Thermo Scientific using a ChemiLux Imager (CsX-1400 M, Intas, Göttingen, Germany) and Gel-Pro Analyzer software (Media Cybernetics, Bethesda, MD).

2.2. HPLC-based quantification of glutathione and its metabolites

Reduced glutathione (GSH) and S-nitrosoglutathione (GSNO) levels were determined by an HPLC method upon derivatization with Ellmann's reagent (5,5′-dithiobis-(2-nitrobenzoic acid), DTNB) as previously described [42,44,45]. Briefly, samples were incubated with 20 mM DTNB for 5 min and stored at −80 °C before measuring the specific DTNB-GSH adduct as well as free nitrothiobenzoate (NTB) via HPLC. 50 μl of these samples were subjected to HPLC analysis on a Jasco HPLC system equipped with an autosampler (described in Ref. [46]) and a C_{18}-Nucleosil 100–3 (125 × 4 mm) reversed phase column (Macherey & Nagel, Düren, Germany). The mobile phase consisted of component (**A**) citric acid buffer (50 mM, pH 2) and component (**B**) acetonitrile/water (90:10 v/v%) and the following gradients were applied: 0 min, 0% B; 9 min, 100% B; 10 min 100% B; 10.5 min, 0% B. The flow was 1 ml/ml and all products were detected at 338 nm. Typical retention times were 3.6 min for GSNO, 4.8 min for the DTNB-GSH adduct and 6.2 min for the free NTB. Quantification was performed using standards from incubations of DTNB (20 mM) with GSH (10 or 100 μM) as well as commercial GSNO (fresh stock solutions) from Sigma-Aldrich (Deisenhofen, Germany).

2.3. Isocitrate dehydrogenase (ICDH) activity assay

ICDH (porcine, $NADP^+$-dependent; 0.4 U/0.5 ml or 0.656 μM final concentration = 20 μg total protein per reaction vial) (Sigma-Aldrich, Taufkirchen, Germany) in Tris buffer (20 mM), pH 7.4, containing $MnSO_4$ (2 mM), was treated with the $^\bullet NO$-donor Spermine-NONOate (Cayman, Ann Arbor, MI, USA) for 4 h at 37 °C for decomposition ($t_{1/2}$ = 40 min). Before the subsequent addition of xanthine oxidase (from buttermilk) (Sigma) for 2 h, DL-isocitric acid (0.5 mM) (Cayman) was supplemented. ICDH activity was determined by the addition of DL-isocitric acid (4 mM) (Cayman) and $NADP^+$ (0.1 mM) (Carl Roth, Karlsruhe, Germany). The enzymatic reduction of $NADP^+$ to NADPH was spectrophotometrically followed at 340 nm over the course of 20 min in 5 min intervals at 37 °C. The enzymatic activity was determined from the slope of the absorption increase over time. ICDH samples for mass spectrometry analysis were prepared identical.

2.4. Detection of nitric oxide ($^\bullet NO$)

Release of $^\bullet NO$ from S-nitrosoglutathione (Sigma) was detected by an $^\bullet NO$-electrode (Ami NO-700, Innovative Instruments, Tampa, FL, USA) in potassium phosphate buffer (10 mM; pH 7.4) at 37 °C in glass tubes

under constant stirring in a volume of 1 ml [47]. The electrode was calibrated every day with $NaNO_2$ in 0.1 M H_2SO_4 and potassium iodide (0.1 mM). The current difference between base-line buffer signal and the peak following the addition of $NaNO_2$ served for calibration of the instrument.

2.5. Assessment of peroxynitrite formation

Dihydrorhodamine 123 displays a preferential detection of peroxynitrite [48]. DHR 123 (1 μM) (Sigma) in potassium phosphate (10 mM), pH 7.4, containing deferoxamine (100 μM) (Sigma) to prevent Fenton chemistry, was treated with S-nitroso-ʟ-glutathione (GSNO) (Cayman), together with xanthine oxidase (from buttermilk, Sigma), DMNQ (Cayman), or KO_2 (Sigma). KO_2 stock solution (100 mM) was prepared in DMSO and added as droplet to the inner dry surface of a reaction tube containing all other components. To initiate the reaction, the tube was gently closed and rapidly vortexed.

2.6. Glutathione detection by enzymatic recycling assay

For the detection of total glutathione (GSH and GSSG), samples (30 μl) were transferred to a 96-well plate and supplemented with 70 μl H_2O. The recycling reaction was initiated by the addition of reaction buffer (sodium phosphate, 100 mM, pH 7.4), containing EDTA (1 mM), 5,5′-dithiobis (2-nitrobenzoic acid) (DTNB) (100 μM) (Sigma), NADPH (100 μM) (Carl Roth), and glutathione reductase (1 U/ml; from baker's yeast) (Sigma). A standard curve with GSH (from 0 μM to 10 μM) was prepared in parallel. After 5 min, DTNB-thiol interaction was analyzed at 405 nm. For the detection of GSSG, a share of the samples was treated first with 2-vinylpyridine in a 20:1 (sample: 2-VP) stoichiometry for 1 h at RT for scavenging of reduced GSH. A GSSG standard curve was prepared (from 0 μM to 10 μM), the samples were then analyzed as described above. To obtain GSH values, oxidized glutathione (GSSG) results were subtracted from total glutathione (GSH + GSSG) values.

2.7. Cell culture

LUHMES are conditionally immortalized human fetal ventral mesencephalic neuronal precursor cells that can be differentiated into neurons with a dopaminergic phenotype [49,50]. Cell culture plates (Sarstedt, surface:Standard) were coated with poly-ʟ-ornithine (50 μg/ml) and fibronectin (1 μg/ml) (Sigma) over night and washed 2x with H_2O. The cells are propagated in Advanced DMEM/F12 medium (Invitrogen), supplemented with 1x N2 (Invitrogen), ʟ-glutamine (2 mM) (Invitrogen), and recombinant basic FGF (R + D Systems) (40 ng/ml). The 2-step differentiation is initiated by Advanced DMEM/F12, containing 1x N2, ʟ-glutamine (2 mM), dibutyryl-cAMP (1 mM) (Sigma), tetracycline (1 μg/ml) (Sigma), and recombinant human GDNF (R + D Systems) (2 ng/ml) for 2 days in cell culture flasks. In this stage, cells ceased proliferation. Cells were then detached by Trypsin (0.05%, Gibco) and a cell density of 180.000 cells/cm^2 was seeded and differentiated for additional 4 days.

2.8. Intracellular DHR 123 oxidation

For the detection of intracellular peroxynitrite formation, LUHMES (180.000 cells/cm^2) in a 96-well plate were treated with •NO-donors for 3 h, followed by the treatment with DMNQ (Cayman), together with DHR 123 (2 μM) for 30 min. Rhodamine fluorescence (λ_{ex} 485 nm; λ_{em} 532 nm) was detected by a Tecan Infinite 200 plate reader.

2.9. Nitration of cellular proteins

As an alternative marker for peroxynitrite formation in intact cells, LUHMES (in 6-well plates; 180.000 cells/cm^2) were treated with •NO-donors for 3 h, followed by the addition of the redox cycler DMNQ for 1

h. Cells were washed with PBS, collected in RIPA buffer and sonicated. Samples (70 μl of a 1 mg/ml solution) were transferred on a PBS-preincubated nitrocellulose membrane (0.45 μm) (Schleicher & Schuell) by a 96-well Dot Blot device (DHM 96; SCIE-PLAS, Cambridge, UK). The membrane was washed in PBS and dried at ambient air for 30 min. The membrane was then blocked with 5% milk powder in PBS-Tween for 2 h, followed by incubation with the primary antibody (anti 3-nitrotyrosine; 1:250, HBT, HM 5001, Uden, The Netherlands) over night. Following 4x washing steps in PBS-Tweeen for 20 min, the membrane was treated with a secondary HRP-conjugated antibody (goat-anti-mouse IgG; Jackson Immuno Research 1:2000). Following washing of the membrane, luminescence was detected and quantified by a Fusion FX system and Bio1D software.

2.10. DMPO dot blot for protein-SNO

Samples from reactions described in 2.3 were used for further immune spin trapping analysis. 20 mM 5,5-dimethyl-1-pyrrolin-N-oxide (DMPO) was added and samples were illuminated with visible light with a wavelength of >420 nm for 30 min. Upon light irradiation, S-nitrosothiols underwent photolytic homolysis. The resulting thiyl radicals were converted to stable thionitrone products using DMPO [51]. Protein-DMPO adducts, representing S-nitros (yl)ation of protein cysteine groups, were quantified by dot blot analysis using a DMPO-specific mouse monoclonal antibody (1:1,000, Stress Marq Biosciences, Canada) according to the established protocols [52,53]. The secondary antibody was a peroxidase-labeled (GAM-POX, 1:2,000, Cell Signaling, Danvers, MA, USA). ECL development was performed as described above in 2.1.

2.11. Mass spectrometric identification of S-nitrosated cysteine residues in the purified isocitrate dehydrogenase (ICDH)

Samples from reactions described in 2.3 were used for further mass spectrometric analysis. All reactions were conducted in orange Eppendorf tubes to limit photo-dissociation. To 250 μl of the reaction, 50 μl of 10% SDS, 200 mM N-ethylmaleimide in water were added. The samples were heated to 50 °C for 1 h. The proteins were subsequently precipitated by adding 1.2 ml of ice-cold acetone. Samples were kept at −20 °C over-night and washed with 100 μl ice-cold acetone. The protein pellets were dried for 15 min and dissolved in a 50 μl of 50 mM Tris pH 8.5, Ascorbate 20 mM, 50 mM iodacetamide, 2 M urea 1 μg of mass spectrometry-grade porcine trypsin (Promega) and incubated a 20 °C for 1 h and 37 °C for 3 h in the dark. Samples were acidified to 0.5% TFA (final concentration) and desalted using stage-tips as previously described [54]. 1 μg of de-salted peptides were loaded onto a 50 cm emitter packed with 1.9 μm ReproSil-Pur 200 C18-AQ (Dr Maisch, Germany) using a RSLC-nano uHPLC systems connected to a Fusion Lumos mass spectrometer (both Thermo, UK). Peptides were separated by a 40 min linear gradient from 5% to 30% acetonitrile, 0.05% acetic acid. Mass spectrometer was operated with a 1 s loop, 60k MS resolution and 30k MS/MS resolution. Data analysis was done using MSFragger [55] embedded in the FragPipe 17.1 using the LFQ-phospho workflow where cysteine variable modification were set to 57.02146 (for carbamidomethylation) or 125.047678 (for N-ethylmaleimidation). Search was conducted against the Uniprot UP000008227 database downloaded in 01/2022 (49977 entries, including contaminants). Mass tolerances were determined heuristically (MS 4 ppm, MS/MS 7 ppm). If no value/peptide were identified across all three replicates we converted the value to a 0 as one can assume that the intensity would be below detection limit, or close to true 0. If one value of the three was missing, we treated the value as missing stochastically and treated it as absent.

2.12. Statistical analysis

Values are expressed as mean ± SD. Experiments were performed at

least three times with at least three technical replicates in each experiment. Differences were tested for significance by one-way or two-way ANOVA, followed by Bonferroni's post hoc test. If not otherwise indicated, differences between means were considered statistically significant at p < 0.05. Two-way ANOVA (with correction for comparison of multiple means) was used for concentration-response data of GSNO and GSH (measured by HPLC). Statistical differences were tested using GraphPad Prism 8.3 (GraphPad Software, La Jolla, USA).

3. Results

3.1. Reductive decomposition of S-nitrosoglutathione

S-nitrosoglutathione (GSNO) was selected as biological relevant

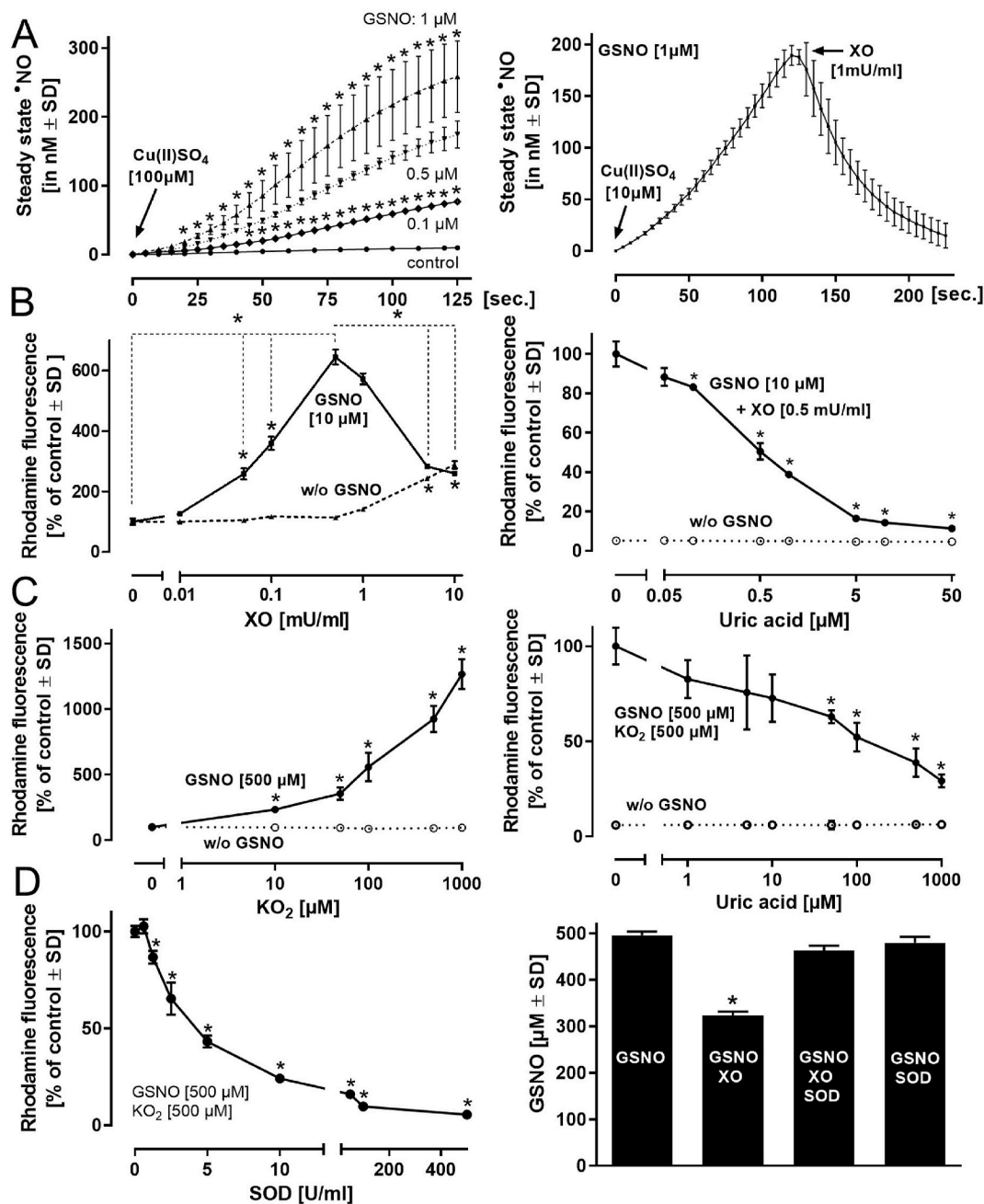**Fig. 1. Release of •NO from nitrosoglutathione and formation of peroxynitrite. A)** S-Nitrosoglutathione (GSNO) in the concentrations as indicated was treated with Cu(II)SO₄, steady–state levels of •NO were assessed by an •NO-sensitive electrode. Selectivity of •NO detection was confirmed by the addition of the superoxide-generating enzyme xanthine oxidase (XO) (+ hypoxanthine 100 μM), resulting in the formation of peroxynitrite. **B)** GSNO was treated with varying activities of XO in the presence of hypoxanthine (500 μM). DHR123 (5 μM) was applied as readout based on its preferential oxidation by peroxynitrite. The peroxynitrite-scavenger uric acid was added to a combination of GSNO (10 μM) and XO (0.5 mU/ml, hypoxanthine 500 μM) for a period of 15 min. **C)** GSNO was treated with varying concentrations of KO₂ from a stock in DMSO. DHR123 (5 μM) was applied as readout based on its preferential oxidation by peroxynitrite. The peroxynitrite-scavenger uric acid was added to a combination of GSNO (500 μM) and KO₂ (500 μM). **D)** To illustrate the direct interaction of O₂•⁻ with nitrosothiols, GSNO (500 μM) was treated with KO₂ (500 μM) in the presence of varying activities of superoxide dismutase (SOD). Likewise, GSNO content of a 500 μM solution was followed by photospectrometry at 335 nm (ε = 922 M⁻¹cm⁻¹), following its incubation with XO (1 mU/ml) in the presence and absence of SOD (100 U/ml) for 4 h. Values are means of 3 independent experiments ±SD. Differences were tested for significance by one-way ANOVA, followed by Bonferroni's post hoc test. *p < 0.05 for comparison with controls.

model for the investigation of non-enzymatic de-nitrosation reactions. We could confirm $^{\bullet}$NO release from GSNO by reduced Cu^{+} as reported previously [35]. Interestingly, also Cu^{2+} (Fig. 1A) allowed an efficient $^{\bullet}$NO release. The same phenomenon has been described in the literature [37] and could be attributed to a contamination of GSNO with GSH, responsible for the reduction of Cu^{2+} to Cu^{+}. To confirm the nature of the detected $^{\bullet}$NO signal and the selectivity of the $^{\bullet}$NO electrode, superoxide ($O_2^{\bullet-}$)-generating xanthine oxidase (XO) (and its substrate hypoxanthine) was added during $^{\bullet}$NO release and resulted in a drop of free $^{\bullet}$NO (Fig. 1A) by the interaction of $^{\bullet}$NO and $O_2^{\bullet-}$ to form peroxynitrite. In order to investigate the hypothesis of $O_2^{\bullet-}$ as potential non-enzymatic denitrosation mechanism, xanthine oxidase (XO) was employed as $O_2^{\bullet-}$ source. $O_2^{\bullet-}$ dependent release of $^{\bullet}$NO from GSNO leads to the subsequent formation of peroxynitrite, hence dihydrorhodamine 123 (DHR 123) oxidation was chosen as readout, as this dye has been elaborated to display a preferential detection of peroxynitrite over other reactive oxygen- and nitrogen species. A concentration-dependent increase in DHR 123 oxidation could be observed (Fig. 1B). Formation of peroxynitrite was further substantiated by the addition of the selective peroxynitrite-scavenger uric acid that indicated a concentration-dependent decline of GSNO/$O_2^{\bullet-}$ evoked peroxynitrite formation (Fig. 1B). The findings made with $O_2^{\bullet-}$ generating XO was corroborated by the use of KO_2 (Fig. 1C). DHR 123 oxidation in the presence of GSNO increased upon addition of KO_2, which was prevented by uric acid in a concentration-dependent manner (Fig. 1C). Of note,

denitrosation and subsequent peroxynitrite formation from the interaction of GSNO and KO_2 was prevented by increasing concentrations of SOD (Fig. 1D). Photospectrometrical detection of GSNO confirmed the denitrosation of GSNO by $O_2^{\bullet-}$, which could be prevented in the presence of SOD (Fig. 1D).

3.2. Restoration of reduced thiol from the interaction of GSNO and $O_2^{\bullet-}$

The formation of peroxynitrite from nitrosothiols and $O_2^{\bullet-}$ raises the question on the fate of the thiol group. GSNO was treated with Cu^{+} or Cu^{2+} as GSNO decomposition catalyst, respectively with XO as $O_2^{\bullet-}$ generating system. Following complete consumption of the XO substrate hypoxanthine/xanthine, and consequently the termination of $O_2^{\bullet-}$ formation, the samples were analyzed for the respective content of reduced (GSH) and oxidized (GSSG) glutathione. GSH and GSSG were detected by the enzymatic recycling assay (Fig. 2A). To corroborate these findings, the consumption of GSNO and formation of reduced GSH was additionally analyzed by HPLC (Fig. 2B-C). When a fixed concentration of GSNO was used, its concentration started to decline upon addition of 0.66 mU/ml of XO with simultaneous formation of GSH. Measurement of GSH levels indicated a high background of basal GSH levels that either represent a contamination of the GSNO stock solution or is formed by alternative mechanisms, e.g. by light-triggered homolysis of GSNO. This became even clearer, when a fixed dose of 4 mU/ml of XO was incubated with increasing concentrations of GSNO, which resulted in a linear
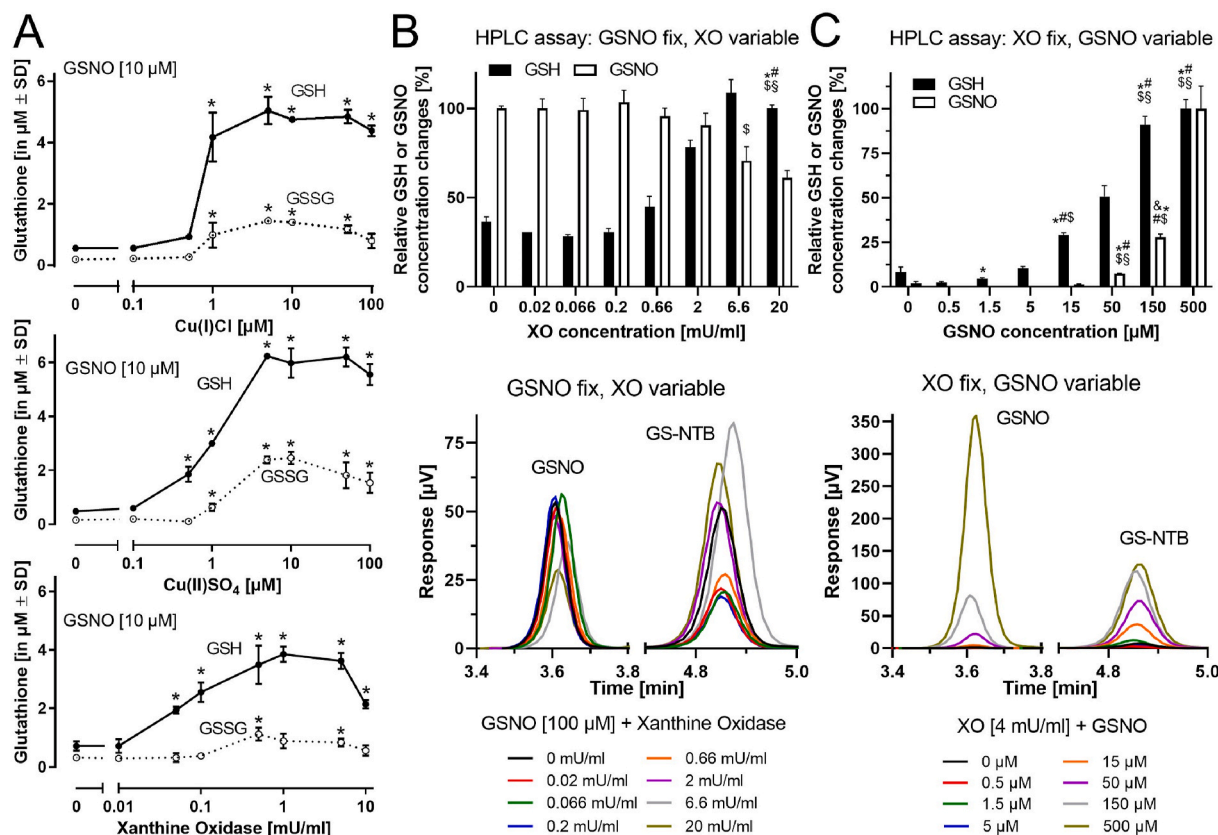

Fig. 2. Products of GSNO reduction. *A)* GSNO (10 μM) was treated with $O_2^{\bullet-}$ generating XO, respectively with Cu(I) or Cu(II) for 4 h. Reduced (GSH) and oxidized (GSSG) glutathione were assessed by the DTNB/glutathione reductase recycling assay. ***B)*** As alternative readout, GSNO and GSH-DTNB adduct were assessed by HPLC. GSNO (100 μM) was treated with variable activities of XO. ***C)*** vice versa, XO (4 mU/ml) was treated with different concentrations of GSNO. Values are means of 3 independent experiments ± SD. (A) Differences were tested for significance by one-way ANOVA, followed by Bonferroni's multiple comparisons test. *$p < 0.05$ for comparison with controls. (B) Differences were tested for significance by repeated measures 2-way ANOVA, followed by Šídák's multiple comparisons test. $p < 0.05$ indicated by * vs. 0.02, # vs. 0.066, $ vs. 0.2, § vs. 0.66 mU/ml XO. (C) Differences were tested for significance by repeated measures 2-way ANOVA, followed by Šídák's multiple comparisons test. $p < 0.05$ indicated by & vs. 0, * vs. 0.15, # vs. 0.5, $ vs. 1.5, § vs. 5. Of note, there was a limitation of the HPLC analysis as reflected by appreciable background GSH signals. Accordingly, these data are only presented as relative changes (% of GSH or GSNO) reflecting the qualitative changes in support of the concept.

increase in GSH until a concentration of GSNO of 150 μM, obviously reflecting a plateau. Contrary to the expectation of oxidized glutathione formation, both methods confirmed the generation of reduced glutathione (GSH) as the major product both in copper- and $O_2^{\bullet-}$ mediated de-nitrosation of GSNO (Fig. 2). Regarding the efficacy of the denitrosation reaction, approximately 40% of the GSNO were denitrosated at a GSNO: $O_2^{\bullet-}$ ratio of roughly 1:1.5 (Fig. 2B). This was based on an estimated $O_2^{\bullet-}$ formation rate of 3440 nM/min by 20 mU/ml XO and 1 mM HX for a total incubation time of 45 min using the published $O_2^{\bullet-}$ formation rate in Ref. [56].

3.3. Switch from S-nitrosation to tyrosine-nitration by $O_2^{\bullet-}$ in albumin

Considering the situation in a cell, the question on the influence of peroxynitrite, generated from the interaction of GSNO and $O_2^{\bullet-}$, emerged. Bovine serum albumin (BSA), a protein containing several cysteine and tyrosine residues, was selected as model to investigate a potential switch from S-nitrosation to tyrosine-nitration mediated by $O_2^{\bullet-}$. In a first step, BSA was exposed to the $^{\bullet}$NO-donor PAPA-NONOate under aerobic conditions allowing S-nitrosation of the protein thiols [57]. Following complete PAPA-NONOate decomposition (to exclude an interaction between $^{\bullet}$NO, actively released from PAPA-NONOate, and $O_2^{\bullet-}$ of XO), nitrosated BSA was exposed to variable XO activities. DHR 123 was utilized as indicator for peroxynitrite generation, and exhibited a significant increase in its oxidation with elevated XO activity only in those BSA samples that were nitrosated before (Fig. 3A). To corroborate peroxynitrite as a dominating reactive nitrogen species formed under these conditions, the peroxynitrite scavenger uric acid was employed and prevented DHR 123 oxidation almost completely (Fig. 3B). To exclude interference by residual parent compound, or by NO_2^- or NO_3^- formed under these conditions, PAPA-NONOate was allowed in parallel

to completely decompose, and was then added to BSA. No significant DHR 123 oxidation was observed under these conditions (not shown). As an alternative approach to confirm peroxynitrite formation from the interaction of GSNO and $O_2^{\bullet-}$, antibody-based staining of BSA tyrosine nitration was conducted. Tyrosine nitration of BSA showed a step-wise elevation, when GSNO concentrations were increased in the presence of a constant amount of XO, or likewise, when XO concentrations were increased in the presence of a constant amount of GSNO (Fig. 3 C-D).

3.4. Switch from nitrosation to nitration by $O_2^{\bullet-}$ in cells

The successful nitration of BSA by GSNO in the presence of an $O_2^{\bullet-}$ source indicates an initial release of $^{\bullet}$NO and its subsequent interaction with a second molecule of $O_2^{\bullet-}$ to yield peroxynitrite. To investigate the involvement of this mechanism also in a biological model, neuronal LUHMES cells were first exposed to the $^{\bullet}$NO-donor PAPA-NONOate for a period that ensures its complete decomposition. On the basis of its membrane permeability, the redox cycler DMNQ was selected as intracellular $O_2^{\bullet-}$ source and elicited a significant elevation of DHR 123 oxidation only when cells were exposed to nitrosation conditions before. As control, fully decomposed PAPA-NONOate was added to the cells instead, followed by DMNQ. This setup could not show an increase in DHR 123 oxidation (not shown). In addition, the cells were homogenized after treatment, and analyzed for total nitrated tyrosine content, that revealed a DMNQ-dependent increase in total 3-nitrotyrosine (Fig. 4A). To further substantiate the formation of peroxynitrite from $O_2^{\bullet-}$ dependent de-nitrosation in intact cells, LUHMES were incubated with PAPA-NONOate first, followed by the subsequent addition of a fixed concentration of DMNQ together with variable concentrations of the peroxynitrite scavenger uric acid. Both DHR123 oxidation, and analysis of total cellular protein nitration, indicated a concentration-
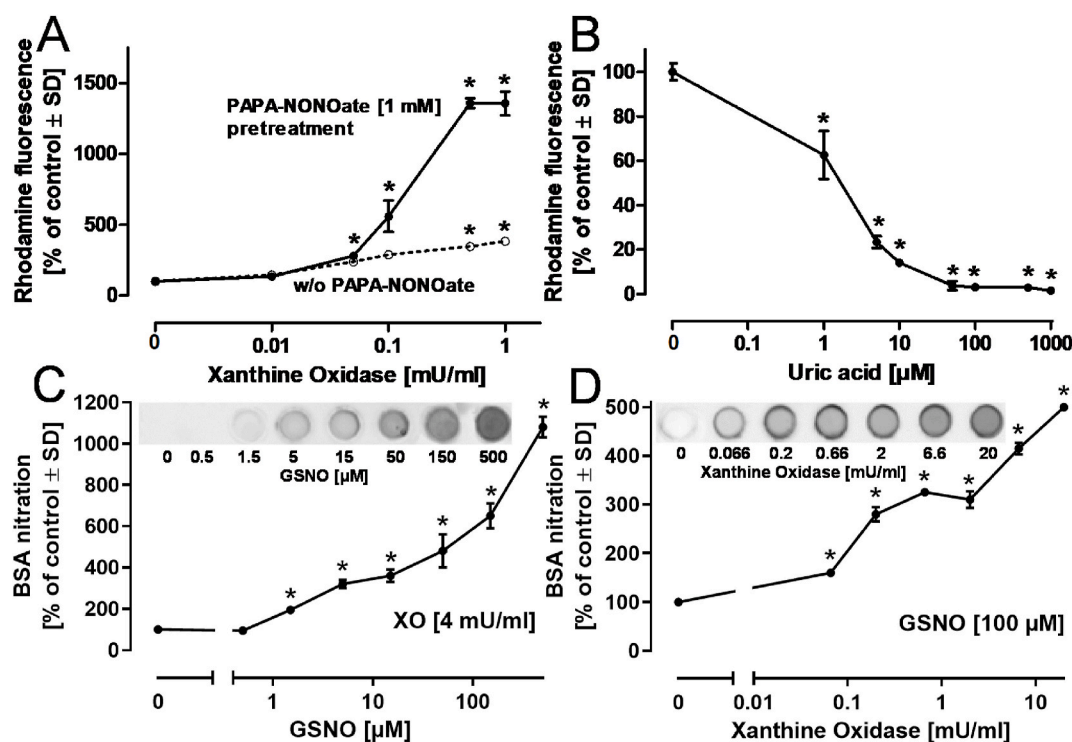

Fig. 3. Protein nitration by GSNO and $O_2^{\bullet-}$. A) Bovine serum albumin (BSA) (1 mg/ml) was pre-treated with the $^{\bullet}$NO-donor PAPA-NONOate (1 mM) for 3 h at 37 °C to ensure complete PAPA-NONOate decomposition. The protein was then incubated with varying activities of XO in the presence of DHR123 (5 μM). B) BSA, pre-treated with PAPA-NONOate (1 mM) for 3 h was incubated with XO (1 mU/ml) in the presence of DHR123 (5 μM) and variable concentrations of the peroxynitrite scavenger uric acid. C) BSA (1 mg/ml) was incubated with different concentrations of GSNO and XO (4 mU/ml + hypoxanthine 500 μM) and stained for 3-nitrotyrosine. D) BSA (1 mg/ml) was incubated with variable activities of XO, hypoxanthine (500 μM), GSNO (100 μM), and stained for 3-nitrotyrosine. Values are means of 3 independent experiments ±SD. Differences were tested for significance by one-way ANOVA, followed by Bonferroni's post hoc test. *$p < 0.05$ for comparison with controls.
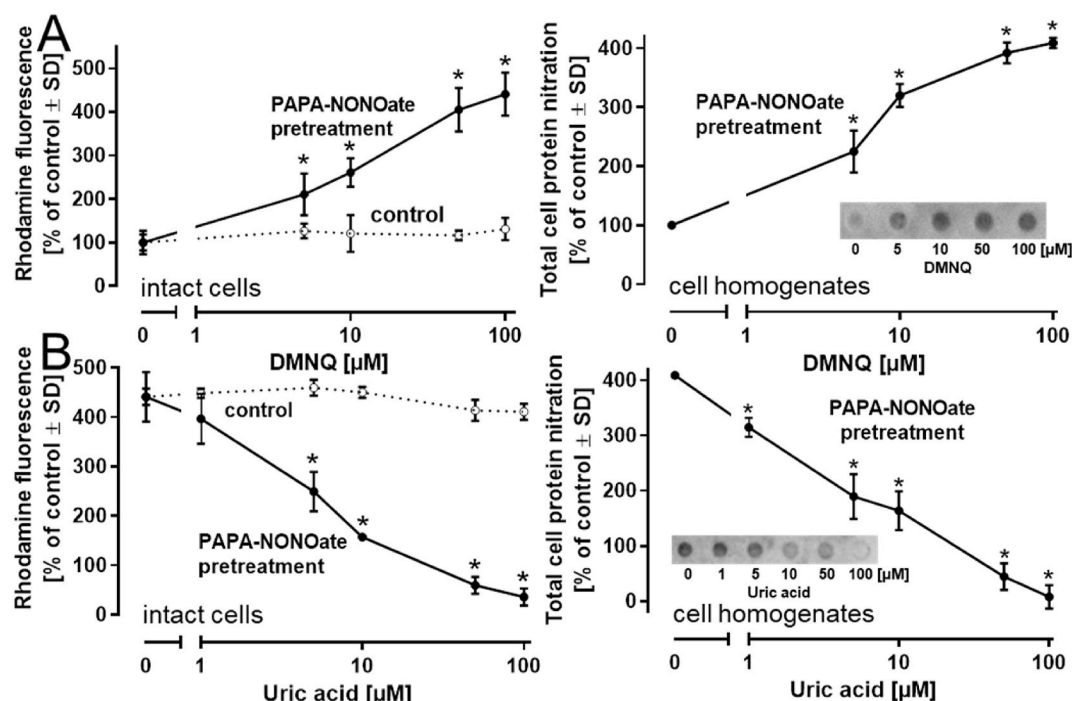
Fig. 4. Nitration of cellular proteins. *A)* LUHMES were pre-treated with PAPA-NONOate (1 mM) for 3 h. The cells were then incubated with the redox cycler DMNQ and with DHR123. For the detection of total protein nitration, cells were homogenized, subjected to dot blot analysis and stained for 3-nitrotyrosine. *B)* LUHMES were pre-treated with PAPA-NONOate (1 mM) for 3h. Then, DMNQ (100 µM) together with varying concentrations of the peroxynitrite-scavenger uric acid were added. Live peroxynitrite formation was detected by following DHR123 oxidation (2 µM), total protein nitration was assessed by 3-nitrotyrosine staining. Values are means of 3 independent experiments ±SD. Differences were tested for significance by one-way ANOVA, followed by Bonferroni's post hoc test. *$p < 0.05$ for comparison with controls.

dependent protection from peroxynitrite by uric acid (Fig. 4B).

3.5. Reversibility of ICDH nitrosation by $O_2^{\bullet-}$

S-nitrosation has been reported in the literature as regulator of a variety of cellular functions, such as GAPDH activity, caspase or HIF-1α inactivation, NF-κB activation, or mitochondrial respiratory chain function [6–8,58,59]. These observations have now raised the issue on a potential role of $O_2^{\bullet-}$ dependent denitrosation and an associated restoration of function. Inhibition of isocitrate dehydrogenase (ICDH) (NADP$^+$-dependent) by nitrosation has previously been reported [60]. Activity of purified porcine ICDH was hence chosen as readout and was determined by the quantification of NADP$^+$ reduction in the presence of its substrate isocitric acid. Treatment of ICDH with the $^\bullet$NO-donor spermine-NONOate (Fig. 5A) or PAPA-NONOate (not shown) resulted in an inhibition of enzyme activity that could be largely reversed by dithiothreitol (DTT). When XO was applied as $O_2^{\bullet-}$ source, a less pronounced, but significant restoration of ICDH activity was observed (Fig. 5A). Reactivation of ICDH was prevented in the presence of SOD. In absence of substrate isocitric acid, as well as with high $O_2^{\bullet-}$ fluxes, inhibition of ICDH activity by $O_2^{\bullet-}$ alone was however observed (Fig. 5B). This $O_2^{\bullet-}$ mediated inactivation could not be reversed by DTT, thus indicating an irreversible oxidation of critical amino acids. This notion is in accordance with moderate tyrosine nitration signals observed by dot blot analysis in these ICDH samples with added spermine-NONOate as well as spermine-NONOate + XO (Fig. 5C). However, 3-nitrotyrosine may also originate from other protein contaminations in the ICDH preparation as our LC-MS analysis identified only nitrated peptides from other proteins but not from ICDH (not shown).

Using the same samples as those used for enzymatic ICDH activity measurements, we found S-nitrosated ICDH enzyme upon incubation with the $^\bullet$NO-donor spermine-NONOate and decreased S-nitrosothiol signal upon incubation with XO or DTT, as envisaged by dot blot analysis

with immune spin trapping (Fig. 5D). Likewise, in the same samples, we identified five S-nitrosated peptides of ICDH upon incubation with spermine NONOate, although one of these peptides was a shorter fragment of another peptide with an additional oxidative modification of methionine (Fig. 6B-C). The intensity of all S-nitrosated peptides was decreased following incubation with XO and three of these S-nitrosated peptides were completely absent in the XO-treated samples (Fig. 6B). For clarification, we detected a surrogate of S-nitrosylated peptides, namely carbamylated peptides (Fig. 6A). These were S-nitrosated peptides that were reduced using ascorbic acid and then the free thiols were alkylated using iodacetamide. In contrast, all free thiols were modified by N-ethylmaleimide in the first step of sample preparation and all other thiol oxidation states are not observed. We would like to stress that our intention was not to globally sequence –SNO sites but to quantify relative changes of –SNO sites across different treatments, only determining differences respective our (negative) treatment controls.

4. Discussion

In the present study, we confirm previous evidence for an $O_2^{\bullet-}$-driven non-enzymatic denitrosation of thiol groups in low-molecular weight biomolecules and extend this concept to a protein, ICDH, also demonstrating rescue of enzymatic activity. As reaction product, most of the thiols were identified in a reduced state while peroxynitrite was formed in parallel.

4.1. Reductive decomposition of S-nitrosoglutathione by superoxide

Cu$^+$-dependent decomposition of GSNO and protein-SNO has been reported previously [35] and could be verified in the present study. Interestingly, $^\bullet$NO release was also observed from GSNO exposure to Cu^{2+}. In agreement with previous reports, we could confirm residual levels of reduced GSH as contamination in the GSNO preparations. GSH
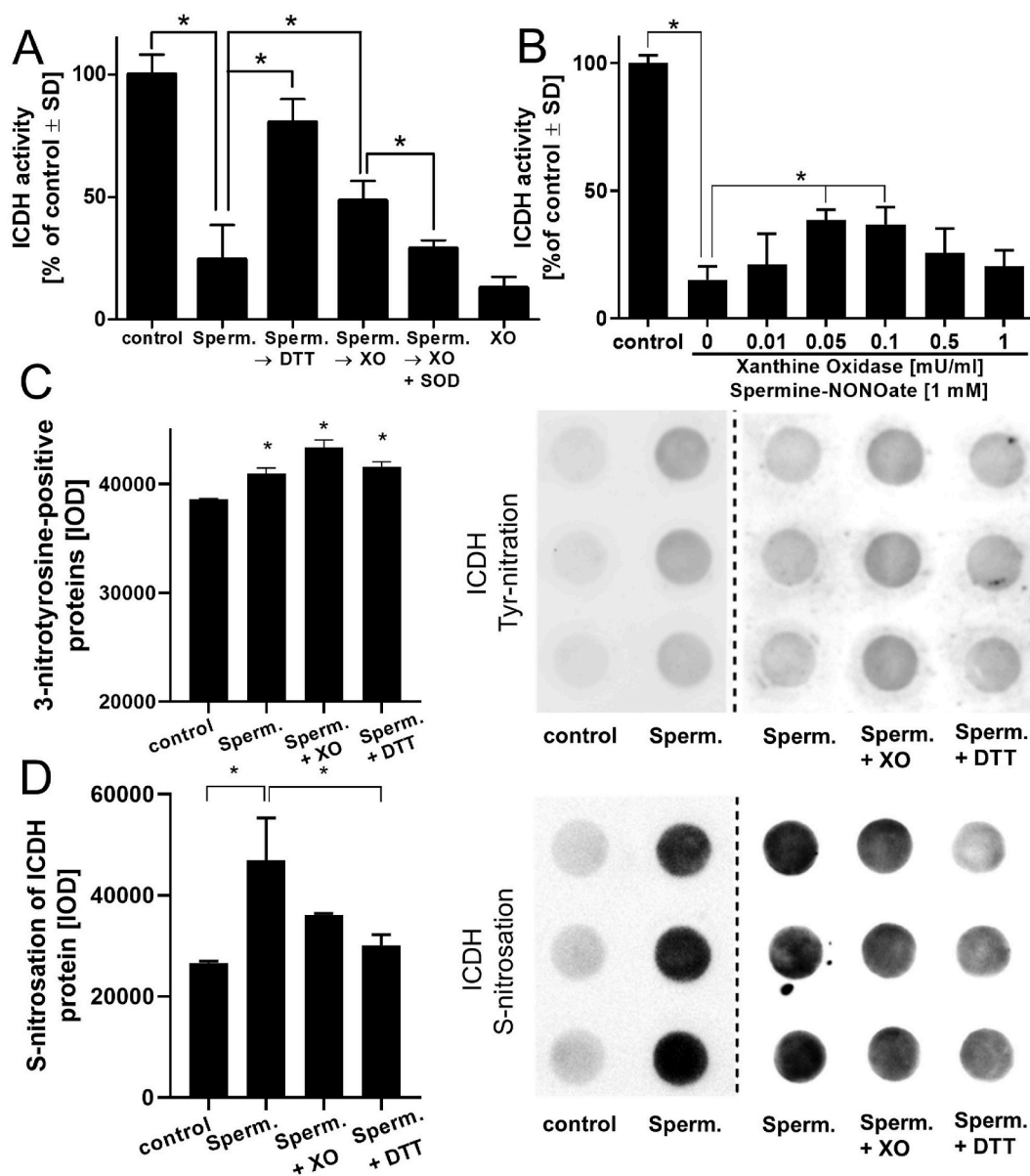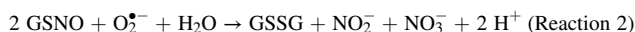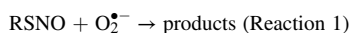
Fig. 5. Reversibility of ICDH nitrosation. *A)* Isocitrate dehydrogenase (ICDH; 0.4 U/500 µl reaction solution) was treated with the $^\bullet$NO-donor spermine-NONOate (Sperm., 1 mM) for a period of 6 h, exposed to air at 37 °C. Then, samples were incubated with dithiothreitol (DTT, 1 mM) or with a mixture of xanthine oxidase (0.1 mU/ml), hypoxanthine (20 µM), together with uric acid (100 µM) or superoxide dismutase (SOD, 50 U/ml) for 1 h. A low concentration of ICDH substrate hypoxanthine was selected to ensure its complete consumption within the incubation period of 1 h. This guarantees the absence of $^\bullet O_2^-$ generation during ICDH activity detection. *B)* ICDH (0.4 U/reaction) was treated with the $^\bullet$NO-donor spermine-NONOate (1 mM) for 6 h for full decomposition. The enzyme was then incubated with varying activities of xanthine oxidase (XO), together with its substrate hypoxanthine (20 µM) for 1 h. ICDH activity was determined by photospectrometrical detection of NADP $^+$ reduction. *C)* 3-nitrotyrosine formation was observed in the ICDH preparation, which however was mostly due to nitration of contaminating proteins in the commercial ICDH preparation (based on LC-MS analysis, not shown). *D)* ICDH S-nitrosation was quantified by dot blot analysis using a DMPO-specific antibody upon immune spin trapping of ICDH-SNO by illumination in the presence of DMPO. As a negative control, the samples were treated with DTT (1 mM). Representative blotting images are shown besides the densitometric quantification. Values are means of 3 independent experiments ±SD. Differences were tested for significance by one-way ANOVA, followed by Bonferroni's post hoc test. *$p < 0.05$ for comparison with controls.

serves as electron source for the reduction of Cu^{2+} to yield Cu^+ as the key catalyst for GSNO decomposition [37]. For cysteine-SNO and for GSNO [38], $O_2^{\bullet-}$ dependent decomposition, according to Reaction 1, was reported to proceed with a rate constant of $1.28 \times 10^4\,M^{-1}s^{-1}$ for GSNO and $7.69 \times 10^4\,M^{-1}s^{-1}$ for cysteine-SNO [39].

$$RSNO + O_2^{\bullet-} \rightarrow products \text{ (Reaction 1)}$$

$$2\,GSNO + O_2^{\bullet-} + H_2O \rightarrow GSSG + NO_2^- + NO_3^- + 2\,H^+ \text{ (Reaction 2)}$$

However, when applying a more complex kinetic model, considering other relevant reactions for the formation of reactants, such as $HO_2^\bullet$, a much slower rate constant of $3 \times 10^2\,M^{-1}s^{-1}$ for GSNO was calculated for Reaction 1 and the authors concluded that direct reaction of superoxide with GSNO plays a minor role under biological conditions as many other reactions are competing, e.g. the disproportionation of $O_2^{\bullet-}$ [38]. This report is however at variance with other work reporting faster rate constants, e.g. 3–$6 \times 10^8\,M^{-2}s^{-1}$ (2nd order for GSNO) in Ref. [40] and $1 \times 10^4\,M^{-1}s^{-1}$ in Ref. [41]. Both of these studies reported the formation of peroxynitrite as a side product of Reaction 1. The major products reported by the first study were GSSG, nitrite and nitrate when GSNO was incubated with XO/HX (Reaction 2) [40]. However, Reaction 2 is not charge balanced, indicating that some important product may be
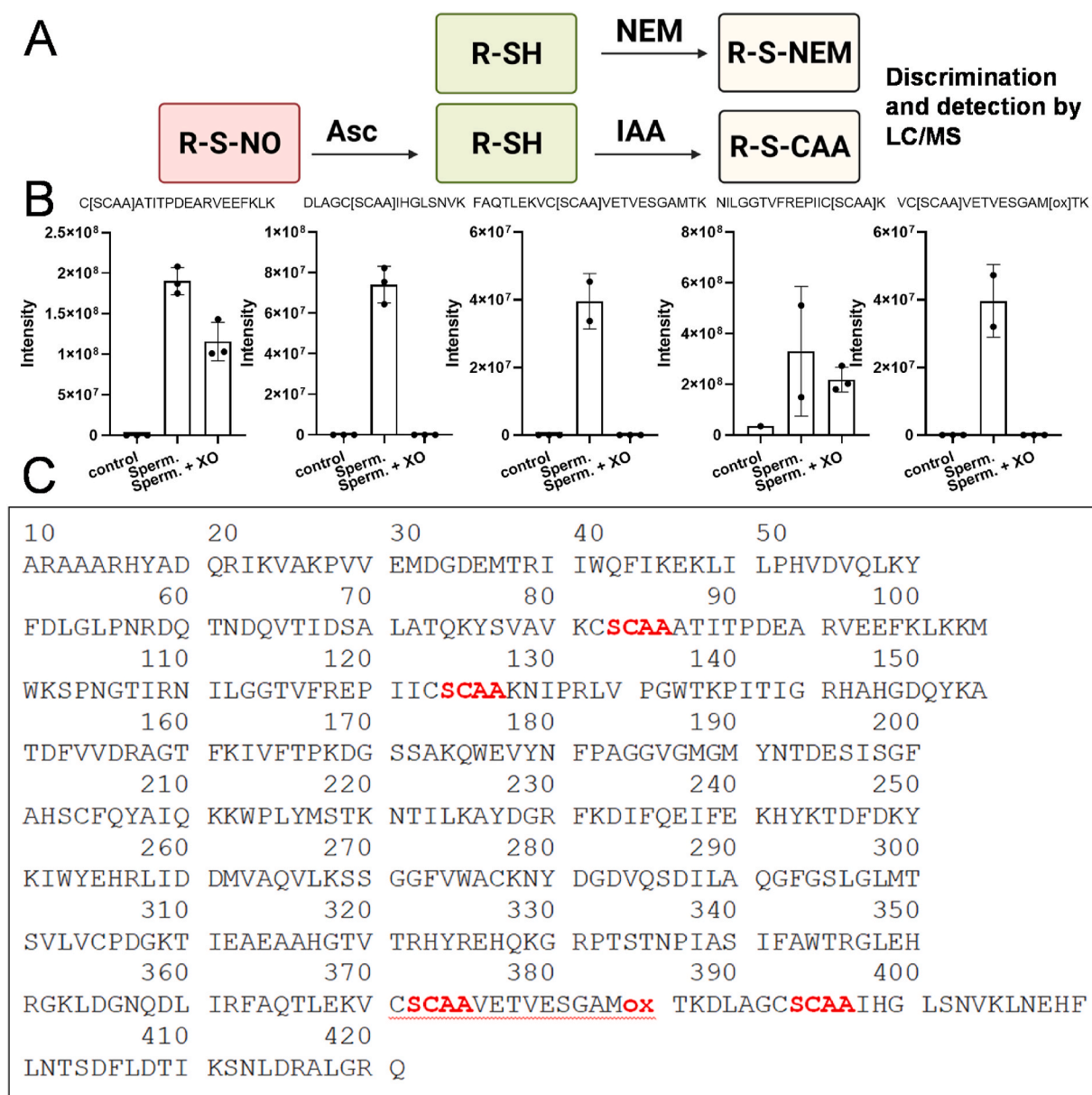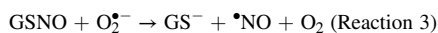
Fig. 6. Reversibility of ICDH nitrosation analyzed by mass spectroscopy. *A)* Methodological scheme of the derivatization and treatment of samples for the LC-MS analysis. First, all reduced thiol groups were alkylated using N-ethylmaleimide (NEM), then all potential S-nitrosated thiols were reduced by ascorbate and alkylated by iodacetamide (IAA) leading to the carbamidomethyl (CAA) product, which was detected by LC-MS. *B)* Identified S-nitrosated and denitrosated peptides from ICDH by LC-MS analysis using the same samples as prepared for experiments in A&B. *C)* S-nitrosated cysteines (carbamidomethyl (CAA) product) in the sequence of porcine ICDH (UniProtKB - P33198). Values are means of 2–3 independent experiments ± SD.

missing here. Accordingly, the major products suggested by the second study were thiolate, $^{\bullet}NO$ and O_2 when GSNO was incubated with XO/HX (Reaction 3), where $^{\bullet}NO$ would directly react with $O_2^{\bullet-}$ to form peroxynitrite (Reaction 4) [41].

$$GSNO + O_2^{\bullet-} \rightarrow GS^- + {^{\bullet}NO} + O_2 \text{ (Reaction 3)}$$

$${^{\bullet}NO} + O_2^{\bullet-} \rightarrow ONOO^- \text{ (Reaction 4)}$$

Our present data show that the reaction of GSNO and superoxide mostly yields reduced GSH (75% of total GSNO) and GSSG as a side product (25% of total GSNO), which would be in accordance with the suggested product pattern in **Reaction 3** [41]. It is surprising that mostly GSH is formed, despite peroxynitrite formation, as indicated by dihydrorhodamine 123 (DHR 123) oxidation (Fig. 1B) and BSA nitration (Fig. 3). Peroxynitrite ($ONOO^-$), with a pK_a of 6.8, is in acid/base equilibrium with peroxynitrous acid (ONOOH). The acid form undergoes homolytic cleavage to form the $^{\bullet}NO_2$ radical and the hydroxyl radical [61–63]. Under conditions of excess of $O_2^{\bullet-}$ over peroxynitrite, as employed in the present work, $O_2^{\bullet-}$ could combine with the $^{\bullet}OH$ radical to form OH^- and O_2, as well as with $^{\bullet}NO_2$ to form peroxynitrate (HNO_4) that is instable and decomposes into nitrate and O_2 [64]. These reactions could contribute to the observed protection of thiolate oxidation from peroxynitrite and $O_2^{\bullet-}$ and hence explain the preferential generation of reduced GSH observed in Fig. 2. Importantly, GSNO denitrosation by XO could be effectively inhibited by superoxide dismutase (SOD), whereas CysSNO denitrosation was only inhibited partially in the presence of SOD [41]. The authors attributed this difference to a direct reaction of CysSNO with XO and inactivation of the enzyme. However, this will probably not affect our ICDH reaction as a direct interaction of the XO active site with the S-nitrosated cysteines of ICDH is rather unlikely due to steric reasons. Inhibition of GSNO denitrosation by XO in the presence

of SOD was also shown previously [40].

4.2. Reversibility of S-nitrosation by $O_2^{\bullet-}$ as mechanism to restore enzymatic activity?

S-nitrosation has been reported in the literature as regulator of a variety of cellular functions, such as GAPDH activity [8,59] or mitochondrial respiratory chain function [65]. These observations have now raised the issue on a potential contribution of $O_2^{\bullet-}$-dependent de-nitrosation and an associated restoration of function in relevant biological targets. Isocitrate dehydrogenase (ICDH; NADP$^+$-dependent) was selected as model system, based on previous reports indicating inactivation by nitrosation [60], inactivation by diamide-induced disulfide bridge formation [66], inactivation by N-ethylmaleimide, associated with an alkylation of multiple cysteine residues [67]. When subjecting ICDH to nitrosating conditions, residues Cys$_{305}$ and Cys$_{387}$ were found to be S-nitrosated [60].

We observed that treatment of ICDH with the NO$^+$ donor sodium nitroprusside, or with GSNO, resulted in an only weak inhibition of the enzyme, while $^\bullet$NO donors such as spermine-NONOate or PAPA-NONOate evoked a concentration dependent decline in enzyme activity. The $^\bullet$NO$_2$ radical, respectively the nitrosating species N$_2$O$_3$, can originate from the autoxidation of $^\bullet$NO [15–18]. As this reaction is second order with respect to $^\bullet$NO, the reaction is considered as too slow for quantitative formation of N$_2$O$_3$. As an alternative explanation, the formation of thiyl radicals was suggested as essential intermediate of S-nitrosation, involving a first order reaction in $^\bullet$NO [20–23]. In the presence of O$_2$, this mechanism provides a mechanistic explanation for the efficient nitrosation of ICDH in the present work by $^\bullet$NO donors. Nitrosation and inhibition of ICDH has also been achieved by the formation of $^\bullet$NO and $O_2^{\bullet-}$ fluxes in a 3:1 ratio as previously reported [14, 68]. The 3:1 ratio can be obtained by modulation of $^\bullet$NO donor concentration on the one side, and adjustment of the activity of the $O_2^{\bullet-}$ source xanthine oxidase on the other. Alternatively, compounds such as Sin-1 that release $^\bullet$NO and concomitantly generate $O_2^{\bullet-}$ in an 1:1 ratio can be applied together with an appropriate activity of superoxide dismutase to yield a 3:1 ratio of $^\bullet$NO: $O_2^{\bullet-}$. These methods however can not guarantee an ideal 3:1 ratio over the entire incubation period and consequently generate other oxidative modifications that can influence the outcome of the study. For this reason, nitrosation by $^\bullet$NO-donors was chosen as method of choice for the experiments of the present work.

In accordance with the literature data, we observed that treatment of ICDH with the $^\bullet$NO-donor spermine-NONOate resulted in an inhibition of enzymatic activity that could be largely reversed by DTT. Also, incubation of the S-nitrosated and inactivated enzyme with XO, as a $O_2^{\bullet-}$ source, led to partial restoration of ICDH activity, which was also mirrored by a decline in the S-nitrosation intensity of different cysteines (Fig. 5). We were able to identify S-nitrosated Cys$_{387}$ (Fig. 6) as described by Yang et al. as the underlying mechanism of $^\bullet$NO-dependent inactivation [60]. Importantly, in our experiments, excess formation of $O_2^{\bullet-}$ caused overoxidation of the non-nitrosated ICDH that could not be reversed by DTT. We made these observations in association with e.g. GAPDH, glutathione reductase, or caspase-3. In all cases mentioned, S-nitrosation resulted in an inhibition of enzyme activity. Reactivation of enzymatic activity by $O_2^{\bullet-}$ mediated denitrosation however failed in these selected examples. While denitrosation by $O_2^{\bullet-}$ actually worked at least partially, oxidative modifications evoked by $O_2^{\bullet-}$, or by peroxynitrite, generated under these conditions, resulted in the actual inhibition of these enzymes, independent from nitrosation-dependent inactivation (data not shown). In addition, even low $O_2^{\bullet-}$ (and resulting H$_2$O$_2$) concentrations may lead to reversible oxidation of thiols (e.g. sulfenic acid, sulfinic acid and disulfides). In contrast to the situation in GSH, thiols in proteins are often located in environments that support a low pK$_a$. Thiols with low pK$_a$ values are more prone to oxidative modifications due to a higher degree of ionization at physiological pH [69]. These considerations could explain the observed differences in denitrosation of thiols in

GSH, respectively in enzymes. It also illustrates the significant influence of the individual environment of a thiol on its susceptibility towards $O_2^{\bullet-}$ dependent irreversible inactivation, or reactivation by denitrosation.

As a limitation of the study, we have to state that different GSNO batches of potentially different purity were used (photometric quantification of the last batch revealed a purity of >95%). This could have been a source of overestimation of the GSNO concentrations in the reaction solutions of the experimental groups. We also noticed a GSH contamination of the GSNO stock solutions of approximately 3%. Also handling of the GSNO solutions under light irradiation could have led to photochemical decomposition of GSNO, which however would have been the case in the controls as well as KO$_2$ or XO containing solutions.

5. Conclusions and outlook

In the present work, superoxide ($O_2^{\bullet-}$)-dependent reduction of S-nitrosothiols was identified as non-enzymatic denitrosation mechanism, thereby confirming previously published data. In biological systems, this mechanism could be involved under conditions of excessive $O_2^{\bullet-}$ production, as observed e.g. in reperfusion or in defined stages of inflammatory reactions. Re-activation of nitrosated and inactivated enzymes by $O_2^{\bullet-}$ is observed (e.g. ICDH). However, it can not be regarded as universal mechanism due to $O_2^{\bullet-}$-dependent oxidative modifications of the respective enzymes, often at residues distinct from S-nitrosated cysteines. It could consequently be assumed that for re-activation of nitrosated cellular structures, enzyme-mediated mechanisms, e.g. by the thioredoxin system or by nitrosoglutathione reductase, might prevail. These systems, however, are dependent on the availability of sufficient amounts of reducing equivalents [70,71] as well as on accessibility of S-nitrosated cysteine residues to the denitrosating enzymes. Despite the presence of $O_2^{\bullet-}$ and the formation of peroxynitrite, $O_2^{\bullet-}$-dependent denitrosation of GSNO yielded about 75% reduced glutathione (GSH). The efficacy of the GSNO denitrosation reaction was approximately 40% at a GSNO: $O_2^{\bullet-}$ ratio of roughly 1:1.5, which came close to a reported 12.5% denitrosation at a GSNO: $O_2^{\bullet-}$ ratio of roughly 1:1 (16.7% denitrosation of CysSNO when incubated with equimolar $O_2^{\bullet-}$) [39]. However, at higher $O_2^{\bullet-}$ formation rates reversible and irreversible thiol oxidation could be initiated by $O_2^{\bullet-}$, H$_2$O$_2$ or by peroxynitrite formed during denitrosation, which is also reflected by the only partial recovery of ICDH activity. This also implies that the non-enzymatic denitrosation may only play a role in a quite narrow $O_2^{\bullet-}$ concentration range, which may hamper its application to a broad set of biological conditions. Conditions favoring nitrosation, followed by the generation of large fluxes of $O_2^{\bullet-}$, are hallmarks of ischemia-reperfusion. Following nitrosation in ischemia, reperfusion is characterized by fast consumption of reducing equivalents and pronounced formation of $O_2^{\bullet-}$. It could hence be speculated that reduction of GSNO by $O_2^{\bullet-}$ to replenish the pool of cellular GSH could act as determinant in the cell's fate into reconvalescence or death. The adverse side of the proposed mechanism may be the superoxide-driven denitrosation of S-nitrosocaspase isoforms, which would explain the pro-apoptotic effects of oxidative stress, especially of superoxide formation.

Data availability

Data will be made available on request.

Acknowledgments

References

[1] B.C. Smith, M.A. Marletta, Mechanisms of S-nitrosothiol formation and selectivity in nitric oxide signaling, Curr. Opin. Chem. Biol. 16 (5–6) (2012) 498–506.

[2] S.L. Wynia-Smith, B.C. Smith, Nitrosothiol formation and S-nitrosation signaling through nitric oxide synthases, Nitric Oxide 63 (2017) 52–60.

[3] D.A. Wink, J.A. Cook, S.Y. Kim, Y. Vodovotz, R. Pacelli, M.C. Krishna, A. Russo, J. B. Mitchell, D. Jourd'heuil, A.M. Miles, M.B. Grisham, Superoxide modulates the oxidation and nitrosation of thiols by nitric oxide-derived reactive intermediates. Chemical aspects involved in the balance between oxidative and nitrosative stress, J. Biol. Chem. 272 (17) (1997) 11147–11151.

[4] A.J. Gow, Q. Chen, D.T. Hess, B.J. Day, H. Ischiropoulos, J.S. Stamler, Basal and stimulated protein S-nitrosylation in multiple cell types and tissues, J. Biol. Chem. 277 (12) (2002) 9637–9640.

[5] H.E. Marshall, J.S. Stamler, Inhibition of NF-kappa B by S-nitrosylation, Biochemistry 40 (6) (2001) 1688–1693.

[6] Z.T. Kelleher, A. Matsumoto, J.S. Stamler, H.E. Marshall, NOS2 regulation of NF-kappaB by S-nitrosylation of p65, J. Biol. Chem. 282 (42) (2007) 30667–30672.

[7] M.R. Hara, N. Agrawal, S.F. Kim, M.B. Cascio, M. Fujimuro, Y. Ozeki, M. Takahashi, J.H. Cheah, S.K. Tankou, L.D. Hester, C.D. Ferris, S.D. Hayward, S. H. Snyder, A. Sawa, S-nitrosylated GAPDH initiates apoptotic cell death by nuclear translocation following Siah1 binding, Nat. Cell Biol. 7 (2005) 665–674.

[8] S. Mohr, J.S. Stamler, B. Brune, Posttranslational modification of glyceraldehyde-3-phosphate dehydrogenase by S-nitrosylation and subsequent NADH attachment, J. Biol. Chem. 271 (1996) 4209–4214.

[9] J.B. Mannick, C. Schonhoff, N. Papeta, P. Ghafourifar, M. Szibor, K. Fang, B. Gaston, S-Nitrosylation of mitochondrial caspases, J. Cell Biol. 154 (6) (2001) 1111–1116.

[10] L. Rössig, B. Fichtlscherer, K. Breitschopf, J. Haendeler, A.M. Zeiher, A. Mülsch, S. Dimmeler, Nitric oxide inhibits caspase-3 by S-nitrosation in vivo, J. Biol. Chem. 274 (11) (1999) 6823–6826.

[11] T.T. Nguyen, M.V. Stevens, M. Kohr, C. Steenbergen, M.N. Sack, E. Murphy, Cysteine 203 of cyclophilin D is critical for cyclophilin D activation of the mitochondrial permeability transition pore, J. Biol. Chem. 286 (2011) 40184–40192.

[12] S.I. Bibli, A. Papapetropoulos, E.K. Iliodromitis, A. Daiber, V. Randriamboavonjy, S. Steven, P. Brouckaert, A. Chatzianastasiou, K.E. Kypreos, D.J. Hausenloy, I. Fleming, I. Andreadou, Nitroglycerine limits infarct size through S-nitrosation of cyclophilin D: a novel mechanism for an old drug, Cardiovasc. Res. 115 (3) (2019) 625–636.

[13] K.A. Broniowska, N. Hogg, The chemical biology of S-nitrosothiols, Antioxidants Redox Signal. 17 (7) (2012) 969–980.

[14] A. Daiber, S. Schildknecht, J. Müller, J. Kamuf, M.M. Bachschmid, V. Ullrich, Chemical model systems for cellular nitros(yl)ation reactions, Free Radic. Biol. Med. 47 (4) (2009) 458–467.

[15] V.G. Kharitonov, A.R. Sundquist, V.S. Sharma, Kinetics of nitrosation of thiols by nitric oxide in the presence of oxygen, J. Biol. Chem. 270 (47) (1995) 28158–28164.

[16] P.C. Ford, D.A. Wink, D.M. Stanbury, Autoxidation kinetics of aqueous nitric oxide, FEBS Lett. 326 (1–3) (1993) 1–3.

[17] D. Jourd'heuil, F.L. Jourd'heuil, M. Feelisch, Oxidation and nitrosation of thiols at low micromolar exposure to nitric oxide. Evidence for a free radical mechanism, J. Biol. Chem. 278 (18) (2003) 15720–15726.

[18] M.G. Espey, D.D. Thomas, K.M. Miranda, D.A. Wink, Focusing of nitric oxide mediated nitrosation and oxidative nitrosylation as a consequence of reaction with superoxide, Proc. Natl. Acad. Sci. U. S. A. 99 (17) (2002) 11127–11132.

[19] M. Keshive, S. Singh, J.S. Wishnok, S.R. Tannenbaum, W.M. Deen, Kinetics of S-nitrosation of thiols in nitric oxide solutions, Chem. Res. Toxicol. 9 (6) (1996) 988–993.

[20] B. Kolesnik, K. Palten, A. Schrammel, H. Stessel, K. Schmidt, B. Mayer, A.C. Gorren, Efficient nitrosation of glutathione by nitric oxide, Free Radic. Biol. Med. 63 (2013) 51–64.

[21] A. Schrammel, A.C. Gorren, K. Schmidt, S. Pfeiffer, B. Mayer, S-nitrosation of glutathione by nitric oxide, peroxynitrite, and (*)NO/O(2)(*-), Free Radic. Biol. Med. 34 (8) (2003) 1078–1088.

[22] E. Madej, L.K. Folkes, P. Wardman, G. Czapski, S. Goldstein, Thiyl radicals react with nitric oxide to form S-nitrosothiols with rate constants near the diffusion-controlled limit, Free Radic. Biol. Med. 44 (12) (2008) 2013–2018.

[23] M.G. Bonini, O. Augusto, Carbon dioxide stimulates the production of thiyl, sulfinyl, and disulfide radical anion from thiol oxidation by peroxynitrite, J. Biol. Chem. 276 (13) (2001) 9749–9754.

[24] R. Sengupta, A. Holmgren, Thioredoxin and thioredoxin reductase in relation to reversible S-nitrosylation, Antioxidants Redox Signal. 18 (3) (2013) 259–269.

[25] C. Klomsiri, P.A. Karplus, L.B. Poole, Cysteine-based redox switches in enzymes, Antioxidants Redox Signal. 14 (6) (2011) 1065–1077.

[26] A. Daiber, S. Daub, M. Bachschmid, S. Schildknecht, M. Oelze, S. Steven, P. Schmidt, A. Megner, M. Wada, T. Tanabe, T. Münzel, S. Bottari, V. Ullrich, Protein tyrosine nitration and thiol oxidation by peroxynitrite-strategies to prevent these oxidative modifications, Int. J. Mol. Sci. 14 (4) (2013) 7542–7570.

[27] C.H. Chen, G.R. Budas, E.N. Churchill, M.H. Disatnik, T.D. Hurley, D. Mochly-Rosen, Activation of aldehyde dehydrogenase-2 reduces ischemic damage to the heart, Science 321 (5895) (2008) 1493–1495.

[28] K.H. Moon, B.J. Kim, B.J. Song, Inhibition of mitochondrial aldehyde dehydrogenase by nitric oxide-mediated S-nitrosylation, FEBS Lett. 579 (27) (2005) 6115–6120.

[29] H.M. Lee, J.W. Choi, M.S. Choi, Role of nitric oxide and protein S-nitrosylation in ischemia-reperfusion injury, Antioxidants 11 (1) (2021) 57.

[30] E.T. Chouchani, C. Methner, S.M. Nadtochiy, A. Logan, V.R. Pell, S. Ding, A. M. James, H.M. Cochemé, J. Reinhold, K.S. Lilley, L. Partridge, I.M. Fearnley, A. J. Robinson, R.C. Hartley, R.A. Smith, T. Krieg, P.S. Brookes, M.P. Murphy, Cardioprotection by S-nitrosation of a cysteine switch on mitochondrial complex I, Nat. Med. 19 (6) (2013) 753–759.

[31] V. Borutaite, A. Budriunaite, G.C. Brown, Reversal of nitric oxide-, peroxynitrite- and S-nitrosothiol-induced inhibition of mitochondrial respiration or complex I activity by light and thiols, Biochim. Biophys. Acta 1459 (2–3) (2000) 405–412.

[32] E. Clementi, G.C. Brown, M. Feelisch, S. Moncada, Persistent inhibition of cell respiration by nitric oxide: crucial role of S-nitrosylation of mitochondrial complex I and protective action of glutathione, Proc. Natl. Acad. Sci. U. S. A. 95 (13) (1998) 7631–7636.

[33] A. Galkin, A.Y. Abramov, N. Frakich, M.R. Duchen, S. Moncada, Lack of oxygen deactivates mitochondrial complex I: implications for ischemic injury? J. Biol. Chem. 284 (52) (2009) 36055–36061.

[34] L.A. Reyes, J. Boslett, S. Varadharaj, F. De Pascali, C. Hemann, L.J. Druhan, G. Ambrosio, M. El-Mahdy, J.L. Zweier, Depletion of NADP(H) due to CD38 activation triggers endothelial dysfunction in the postischemic heart, Proc. Natl. Acad. Sci. USA 112 (37) (2015) 11648–11653, https://doi.org/10.1073/pnas.1505556112.

[35] G. Stubauer, A. Giuffrè, P. Sarti, Mechanism of S-nitrosothiol formation and degradation mediated by copper ions, J. Biol. Chem. 274 (40) (1999) 28128–28133.

[36] R.J. Singh, N. Hogg, J. Joseph, B. Kalyanaraman, Mechanism of nitric oxide release from S-nitrosothiols, J. Biol. Chem. 271 (31) (1996) 18596–18603.

[37] A.C. Gorren, A. Schrammel, K. Schmidt, B. Mayer, Decomposition of S-nitrosoglutathione in the presence of copper ions and glutathione, Arch. Biochem. Biophys. 330 (2) (1996) 219–228.

[38] E. Ford, H.N. Hughes, P. Wardman, The reaction of superoxide radicals with S-nitrosoglutathione and the products of its reductive heterolysis, J. Biol. Chem. 277 (4) (2002) 2430–2436.

[39] S. Aleryani, E. Milo, Y. Rose, P. Kostka, Superoxide-mediated decomposition of biological S-nitrosothiols, J. Biol. Chem. 273 (11) (1998) 6041–6045.

[40] D. Jourd'heuil, C.T. Mai, F.S. Laroux, D.A. Wink, M.B. Grisham, The reaction of S-nitrosoglutathione with superoxide, Biochem. Biophys. Res. Commun. 246 (3) (1998) 525–530.

[41] M. Trujillo, M.N. Alvarez, G. Peluffo, B.A. Freeman, R. Radi, Xanthine oxidase-mediated decomposition of S-nitrosothiols, J. Biol. Chem. 273 (14) (1998) 7828–7834.

[42] M. Oelze, S. Kröller-Schön, S. Steven, E. Lubos, C. Doppler, M. Hausding, S. Tobias, C. Brochhausen, H. Li, M. Torzewski, P. Wenzel, M. Bachschmid, K.J. Lackner, E. Schulz, T. Münzel, A. Daiber, Glutathione peroxidase-1 deficiency potentiates dysregulatory modifications of endothelial nitric oxide synthase and vascular dysfunction in aging, Hypertension 63 (2) (2014) 390–396.

[43] M. Oelze, M. Knorr, R. Schell, J. Kamuf, A. Pautz, J. Art, P. Wenzel, T. Münzel, H. Kleinert, A. Daiber, Regulation of human mitochondrial aldehyde dehydrogenase (ALDH-2) activity by electrophiles in vitro, J. Biol. Chem. 286 (11) (2011) 8893–8900.

[44] L.K. Sha, W. Sha, L. Kuchler, A. Daiber, A.K. Giegerich, A. Weigert, T. Knape, R. Snodgrass, K. Schröder, R.P. Brandes, B. Brüne, A. von Knethen, Loss of Nrf2 in bone marrow-derived macrophages impairs antigen-driven CD8(+) T cell function by limiting GSH and Cys availability, Free Radic. Biol. Med. 83 (2015) 77–88.

[45] S. Kalinovic, P. Stamm, M. Oelze, S. Daub, S. Kröller-Schön, M. Kvandova, S. Steven, T. Münzel, A. Daiber, Comparison of three methods for in vivo

quantification of glutathione in tissues of hypertensive rats, Free Radic. Res. 55 (11–12) (2021) 1048–1061.

[46] S. Kröller-Schön, S. Steven, S. Kossmann, A. Scholz, S. Daub, M. Oelze, N. Xia, M. Hausding, Y. Mikhed, E. Zinssius, M. Mader, P. Stamm, N. Treiber, K. Scharffetter-Kochanek, H. Li, E. Schulz, P. Wenzel, T. Münzel, A. Daiber, Molecular mechanisms of the crosstalk between mitochondria and NADPH oxidase through reactive oxygen species-studies in white blood cells and in animal models, Antioxidants Redox Signal. 20 (2) (2014) 247–266.

[47] S. Schildknecht, R. Pape, N. Müller, M. Robotta, A. Marquardt, A. Bürkle, M. Drescher, M. Leist, Neuroprotection by minocycline caused by direct and specific scavenging of peroxynitrite, J. Biol. Chem. 286 (7) (2011) 4991–5002.

[48] J.P. Crow, Dichlorodihydrofluorescein and dihydrorhodamine 123 are sensitive indicators of peroxynitrite in vitro: implications for intracellular measurement of reactive nitrogen and oxygen species, Nitric Oxide 1 (2) (1997) 145–157.

[49] S. Schildknecht, D. Pöltl, D.M. Nagel, F. Matt, D. Scholz, J. Lotharius, N. Schmieg, A. Salvo-Vargas, M. Leist, Requirement of a dopaminergic neuronal phenotype for toxicity of low concentrations of 1-methyl-4-phenylpyridinium to human cells, Toxicol. Appl. Pharmacol. 241 (1) (2009) 23–35.

[50] D. Scholz, D. Pöltl, A. Genewsky, M. Weng, T. Waldmann, S. Schildknecht, M. Leist, Rapid, complete and large-scale generation of post-mitotic neurons from the human LUHMES cell line, J. Neurochem. 119 (5) (2011) 957–971.

[51] R. Sengupta, T.R. Billiar, D.A. Stoyanovsky, Studies toward the analysis of S-nitrosoproteins, Org. Biomol. Chem. 7 (2) (2009) 232–234.

[52] S. Kröller-Schön, A. Daiber, S. Steven, M. Oelze, K. Frenis, S. Kalinovic, A. Heimann, F.P. Schmidt, A. Pinto, M. Kvandova, K. Vujacic-Mirski, K. Filippou, M. Dudek, M. Bosmann, M. Klein, T. Bopp, O. Hahad, P.S. Wild, K. Frauenknecht, A. Methner, E.R. Schmidt, S. Rapp, H. Mollnau, T. Münzel, Crucial role for Nox2 and sleep deprivation in aircraft noise-induced vascular and cerebral oxidative stress, inflammation, and gene regulation, Eur. Heart J. 39 (38) (2018) 3528–3539.

[53] M. Kuntic, M. Oelze, S. Steven, S. Kröller-Schön, P. Stamm, S. Kalinovic, K. Frenis, K. Vujacic-Mirski, M.T. Bayo Jimenez, M. Kvandova, K. Filippou, A. Al Zuabi, V. Brückl, O. Hahad, S. Daub, F. Varveri, T. Gori, R. Huesmann, T. Hoffmann, F. P. Schmidt, J.F. Keaney, A. Daiber, T. Münzel, Short-term e-cigarette vapour exposure causes vascular oxidative stress and dysfunction: evidence for a close connection to brain damage and a key role of the phagocytic NADPH oxidase (NOX-2), Eur. Heart J. 41 (26) (2020) 2472–2483.

[54] B. Turriziani, A. Garcia-Munoz, R. Pilkington, C. Raso, W. Kolch, A. von Kriegsheim, On-beads digestion in conjunction with data-dependent mass spectrometry: a shortcut to quantitative and dynamic interaction proteomics, Biology 3 (2) (2014) 320–332.

[55] A.T. Kong, F.V. Leprevost, D.M. Avtonomov, D. Mellacheruvu, A.I. Nesvizhskii, MSFragger: ultrafast and comprehensive peptide identification in mass spectrometry-based proteomics, Nat. Methods 14 (5) (2017) 513–520.

[56] P. Wenzel, H. Mollnau, M. Oelze, E. Schulz, J.M. Wickramanayake, J. Müller, S. Schuhmacher, M. Hortmann, S. Baldus, T. Gori, R.P. Brandes, T. Münzel, A. Daiber, First evidence for a crosstalk between mitochondrial and NADPH

oxidase-derived reactive oxygen species in nitroglycerin-triggered vascular dysfunction, Antioxidants Redox Signal. 10 (8) (2008) 1435–1447.

[57] J.S. Stamler, D.I. Simon, J.A. Osborne, M.E. Mullins, O. Jaraki, T. Michel, D. J. Singel, J. Loscalzo, S-nitrosylation of proteins with nitric oxide: synthesis and characterization of biologically active compounds, Proc. Natl. Acad. Sci. U. S. A. 89 (1) (1992) 444–448.

[58] V.V. Sumbayev, A. Budde, J. Zhou, B. Brüne, HIF-1 alpha protein as a target for S-nitrosation, FEBS Lett. 535 (1–3) (2003) 106–112.

[59] L. Molina y Vedia, B. McDonald, B. Reep, B. Brüne, M. Di Silvio, T.R. Billiar, E. G. Lapetina, Nitric oxide-induced S-nitrosylation of glyceraldehyde-3-phosphate dehydrogenase inhibits enzymatic activity and increases endogenous ADP-ribosylation, J. Biol. Chem. 267 (35) (1992) 24929–24932.

[60] E.S. Yang, C. Richter, J.S. Chun, T.L. Huh, S.S. Kang, J.W. Park, Inactivation of NADP(+)-dependent isocitrate dehydrogenase by nitric oxide, Free Radic. Biol. Med. 33 (7) (2002) 927–937.

[61] S. Goldstein, G. Czapski, The reaction of NO. with O2.- and HO2.: a pulse radiolysis study, Free Radic. Biol. Med. 19 (4) (1995) 505–510.

[62] R. Kissner, T. Nauser, P. Bugnon, P.G. Lye, W.H. Koppenol, Formation and properties of peroxynitrite as studied by laser flash photolysis, high-pressure stopped-flow technique, and pulse radiolysis, Chem. Res. Toxicol. 10 (11) (1997) 1285–1292.

[63] G. Merényi, J. Lind, Free radical formation in the peroxynitrous acid (ONOOH)/ peroxynitrite (ONOO-) system, Chem. Res. Toxicol. 11 (4) (1998) 243–246.

[64] D. Jourd'heuil, F.L. Jourd'heuil, P.S. Kutchukian, R.A. Musah, D.A. Wink, M. B. Grisham, Reaction of superoxide and nitric oxide with peroxynitrite. Implications for peroxynitrite-mediated oxidation reactions in vivo, J. Biol. Chem. 276 (31) (2001) 28799–28805.

[65] G.C. Brown, V. Borutaite, Nitric oxide and mitochondrial respiration in the heart, Cardiovasc. Res. 75 (2) (2007) 283–290.

[66] J.A. Garcia, K.I. Minard, A.P. Lin, L. McAlister-Henn, Disulfide bond formation in yeast NAD+-specific isocitrate dehydrogenase, Biochemistry 48 (37) (2009) 8869–8878.

[67] G.E. Smyth, R.F. Colman, Cysteinyl peptides of pig heart NADP-dependent isocitrate dehydrogenase that are modified upon inactivation by N-ethylmaleimide, J. Biol. Chem. 266 (23) (1991) 14918–14925.

[68] A. Daiber, D. Frein, D. Namgaladze, V. Ullrich, Oxidation and nitrosation in the nitrogen monoxide/superoxide system, J. Biol. Chem. 277 (14) (2002) 11882–11888.

[69] D.T. Hess, A. Matsumoto, S.O. Kim, H.E. Marshall, J.S. Stamler, Protein S-nitrosylation: purview and parameters, Nat. Rev. Mol. Cell Biol. 6 (2) (2005) 150–166.

[70] M.C. Lee, M. Velayutham, T. Komatsu, R. Hille, J.L. Zweier, Measurement and characterization of superoxide generation from xanthine dehydrogenase: a redox-regulated pathway of radical generation in ischemic tissues, Biochemistry 53 (41) (2014) 6615–6623.

[71] D.N. Granger, P.R. Kvietys, Reperfusion injury and reactive oxygen species: the evolution of a concept, Redox Biol. 6 (2015) 524–551.